BOLETIN DE LA SOCIEDAD ESPAÑOLA DE
Cerámica y Vidrio
A R T I C U L O

Magnetic properties of the spinel system $Mg_xMn_{3-x}O_4$ $(0 \leq x \leq 2)$

B. MEHDAOUI, O. PEÑA, M. BAHOUT, A.B. ANTUNES, G. MARTINEZ

[1] Sciences Chimiques de Rennes, UMR 6226, Université de Rennes 1, 35042 Rennes, France
[2] GEMA, Centro Universitário FEEVALE, Novo Hamburgo, RS, Brazil
[3] Institute of Physics, UFRGS, Porto Alegre, RS, Brazil

Temperature-dependent studies of the low-field magnetization of the polycrystalline spinel oxide $Mg_xMn_{3-x}O_4$ $(0 \leq x \leq 2)$ are reported. With the use of Lotgering's model, which is equivalent to the Néel's two-sublattice model, a set of molecular field constants λ_{AB}, λ_{BB} and λ_{AA}, has been obtained for $0 \leq x \leq 0.4$ from the fit of χ between T_C and room temperature. Moreover, this model fits consistently the low-temperature canted-spin angles ψ of the B-sublattice. The Curie temperatures T_C, as well as the exchange parameters J_{AB}, J_{BB} and J_{AA}, show that the BB interactions are much greater than AA and AB, which are of the same order, in contrast to the situation usually found in magnetic spinels. As the concentration of the non-magnetic ion Mg^{2+} increases at the tetrahedral site (A), T_C decreases from 42K (for x = 0) while the ferromagnetic behaviour diminishes at the expense of a magnetic frustration, thus highlighting the great influence of the non-magnetic ions located at the A and B-sites on the magnetic order.

Keywords: Yafet-Kittel structure, Lotgering's model, magnetic dilution, frustration, spin glass.

Propiedades magnéticas del sistema espinela $Mg_xMn_{3-x}O_4$ $(0 \leq x \leq 2)$

Se presentan estudios de la variación térmica de la magnetización a bajo campo de espinelas policristalinas de la solución sólida $Mg_xMn_{3-x}O_4$ $(0 \leq x \leq 2)$. Con la utilización del modelo de Lotgering, que equivale al modelo de Néel de dos subredes, se ha obtenido un conjunto de constantes de campo molecular λ_{AB}, λ_{BB} y λ_{AA}, para $0 \leq x \leq 0.4$ a partir del ajuste de χ entre T_C y temperatura ambiente. Además, este modelo ajusta consistentemente los ángulos ψ de espín canteado de la subred B a baja temperatura. La temperatura de Curie T_C, así como los parámetros de canje J_{AB}, J_{BB} and J_{AA}, muestran que las interacciones BB son mucho mayores que las AA y AB que son ambas del mismo orden, en contraste con lo hallado usualmente en espinelas magnéticas. Cuando la concentración del ión no-magnético Mg^{2+}, aumenta en los lugares tetraédricos, T_C decrece desde 42 K (para x = 0), mientras que el comportamiento ferromagnético se debilita a expensas de una frustración magnética, resaltando así la gran influencia de los iones no-magnéticos localizados en lugares A y B, sobre el orden magnético

Palabras clave: estructura Yafet-Kittel, modelo de Lotgering, dilución magnética, frustración, vidrio de espín.

1. INTRODUCTION

Transition metal spinel oxides of formula AB_2O_4 have attracted much attention in the past for their remarkable ferrimagnetic and electrochemical properties. The structure of a direct spinel is usually described by a cubic close-packed arrangement of oxygen ions, with the divalent A cations at the tetrahedral sites, and the trivalent B cations at the octahedral sites. The ferrimagnetic behavior is mainly due to antiferromagnetic interactions between the A-B sublattices (1).

Renewed interest in spinels is due to their unusual magnetic properties. One of the best known examples is Mn_3O_4 whose magnetic structure was investigated in detail by neutron scattering (2). At room temperature, Mn_3O_4 has a tetragonal distorted spinel structure ($I4_1/amd$). The ionic structure is that of a direct spinel, the Mn^{2+} ions occupying the tetrahedral site (A) whereas the Mn^{3+} ions are located at the octahedral site. Because the tetrahedra are not directly connected, the J_{AA} coupling is usually smaller than J_{AB} and J_{BB} (although J_{AA} controls the B sublattice magnetic configuration); the experimental values are J_{AA} = - 4.9K, J_{AB} = -6.8K and J_{BB} = -19.9K (3). Therefore, as the intra- and inter-sublattice interactions are comparable, the collinear magnetic structure of Mn_3O_4 is destabilized (4). Magnetic studies on powder sample (5) and on single crystal (6) showed that the magnetic ordering below T_C ~ 42 K is not collinear or Néel type, but it consists of a canted arrangement of Yafet-Kittel type, discussed in detail by Lotgering (7). Later, the magnetic structure of Mn_3O_4 has been determined by Jensen and Nielsen using neutron diffraction (8). The major features may be summarized as follows. The ionic structure is $(Mn^{2+})_A[Mn_2^{3+}]_BO_4$. As the temperature is lowered below T_C ~ 42 K, the magnetic structure changes as a function of temperature. Thus, between T_C and T ~ 39 K, the magnetic order is apparently ferromagnetic of Néel type. Between 39 K and 33 K, the Mn^{3+} moments at the B-site form

a spiral spin structure with a propagation vector along [010]. Below 33 K, the magnetic structure consists of a canted Yafet-Kittel spin arrangement, as first suggested by Jacobs (5). The moments of Mn^{2+} at the A site are directed along the [010] axis and the moments of the Mn^{3+} ions on the B sites lie in the (100) plane and subdivide into two sets. Each set makes an angle of 69° with respect to the [0-10] axis, so that the resultant moment at the B-site is antiparallel with respect to that of the A sublattice; the magnetic structure is non-collinear (8).

Recently, the complex magnetic behavior of Mn_3O_4 has been explained according to the concept of magnetic frustration (9). In the A tetrahedral sites, antiferromagnetic (AF) interactions do not yield any frustration and magnetic dilution is a simple percolation problem. By contrast, in the B sublattice, AF interactions yield a topological frustration, like in the pyrochlore lattices (10). Magnetic dilution of the B sublattice partly raises the degeneracy, leading to a spin-glass state. When both sublattices contain only magnetic ions, the dominant AF interactions J_{AB} impose a casual ferromagnetic behavior. Therefore, the phase diagram at 0 K may present a great variety of magnetic phases, whose extension is controlled by the concentration of the magnetic atoms and by the strength of the exchange interactions.

A full understanding of the magnetic properties of Mn_3O_4 is far from being reached and substitution of Mn^{2+} ions by non magnetic ions such as Mg^{2+} would shed additional light on the role of the interactions. In this paper we examine the effect of magnetic dilution at the A-site on the magnetic properties of $Mg_xMn_{3-x}O_4$ ($0 \le x \le 2$) and we fit the paramagnetic susceptibility χ in order to understand the evolution of the spin structure below T_C and evaluate the exchange parameters.

2. EXPERIMENTAL

Stoichiometric quantities of $(C_2H_3O_2)_2Mg$, $4H_2O$ (99.99%) and $(C_2H_3O_2)_2Mn$, $4H_2O$ (99.99%, Aldrich) were dissolved in a minimum quantity of distilled water and heated at 90 °C on a hot plate with constant stirring until complete evaporation of water. The mixture was then ground and heated in a furnace at 600 °C for 15h. The resulting powder was then pressed into 13 mm-diameter pellets at 377 MPas and annealed in air for 24h, at 800 °C (for $x > 1.6$) and at 1000°C (for $x \le 1.6$), then allowed to cool down to room temperature at a rate of 1 °C/min. The black, polycrystalline powders were then sintered at 1000 °C. X-ray powder diffraction (XRD) patterns were collected at room temperature on a Siemens D500 diffractometer ($CuK\alpha_1$, $K\alpha_2$ radiations) in 0.02° steps. Magnetization measurements were performed in the range $5\ K \le T \le 300\ K$ after a zero-field cooling (ZFC) process and during a field cooling (FC) process, using a Quantum Design MPMS-XL5 SQUID magnetometer in a static field of 0.05 T.

3. RESULTS AND DISCUSSION

3.1. X-ray Powder Diffraction

Two solid solution domains are evident from the X-ray powder diffraction patterns of $Mg_xMn_{3-x}O_4$, as shown on Fig.1. For $0 \le x \le 0.9$, the crystal structure was refined in the $I4_1/amd$ tetragonal space group, which is the most commonly observed symmetry lowering from cubic space group Fd3m, when a Jahn-Taller ion such as Mn^{3+} is at the octahedral site

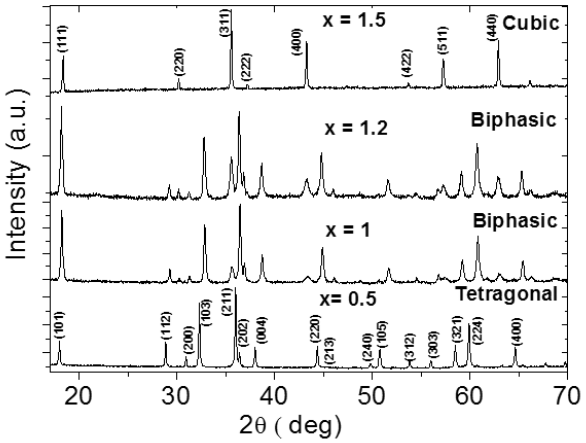

Fig. 1- X-ray diffraction patterns for $Mg_xMn_{3-x}O_4$ (x = 0.5, 1, 1.2, 1.5). Diagramas de difracción de Rayos X para $Mg_xMn_{3-x}O_4$ (x = 0.5, 1, 1.2, 1.5)

and involves the elongation of the octahedra along [001]. In addition, because of different X-ray scattering power of Mg and Mn elements, it was possible to conclude that $Mg_xMn_{3-x}O_4$ ($0 \le x \le 0.9$) are direct spinels with both Mg^{2+} and Mn^{2+} ions at the tetrahedral site. Moreover, the lattice parameters a and c decrease linearly with increasing Mg-content (figure 2-a), in agreement with the Mg-substitution at the A site, as shown also by other authors (11).

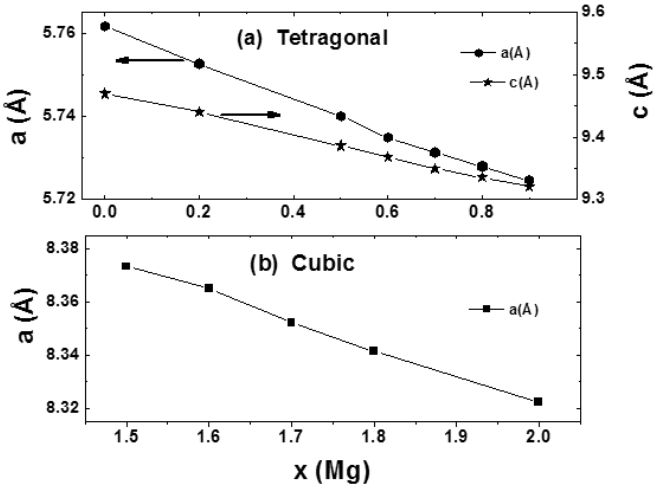

Fig. 2- Variation of lattice constant of $Mg_xMn_{3-x}O_4$ with x: (a) tetragonal domain $0 \le x \le 0.9$, (b) cubic domain $1.5 \le x \le 2$. Variación de la constante de red de $Mg_xMn_{3-x}O_4$ con x: (a) dominio tetragonal $0 \le x \le 0.9$, (b) dominio cúbico $1.5 \le x \le 2$.

For $1.5 \le x \le 2$, the compounds crystallize in the cubic structure, space group Fd3m, with a lattice parameter decreasing linearly with increasing x (figure 2-b). The tetrahedral sites are completely occupied by Mg^{2+} and the additional Mg^{2+} enters the octahedral sites, giving rise to a mixed valence (Mn^{3+}/Mn^{4+}). The structural ionic formula is then $(Mg^{2+})_A[Mg^{2+}_{x-1}Mn^{3+}_{2(2-x)}Mn^{4+}_{x-1}]_BO_4$.

For $1 \le x \le 1.4$, the X-ray patterns show the coexistence of both the tetragonal and cubic phases. In this region the

tetragonal symmetry changes continuously towards cubic when the Mg-content increases, as shown in figure 3.

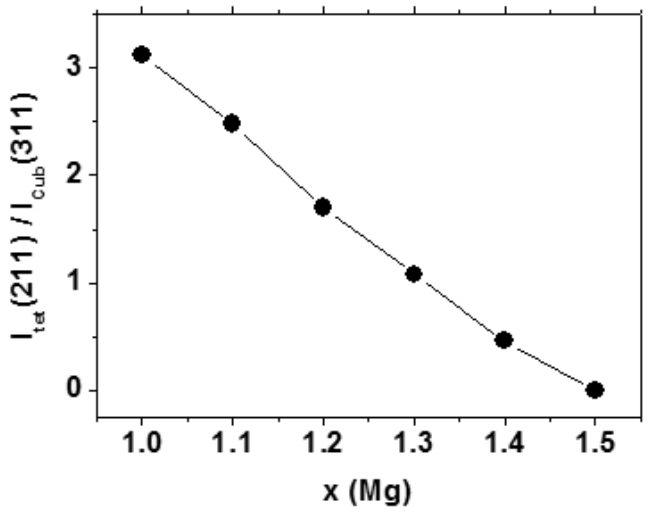

Fig. 3- Evolution of the intensity ratio $I_{tet}(211)/I_{cub}(311)$ with x, for $1 \le x \le 1.5$. Evolución de la razón de intensidad $I_{tet}(211)/I_{cub}(311)$ con x, para $1 \le x \le 1.5$.

3.2. Magnetic Properties

3.2.1. Tetragonal domain $0 \le x \le 0.9$

The inverse molar susceptibilities χ^{-1}, measured at 1 kOe for samples $Mg_xMn_{3-x}O_4$, x = 0, 0.2 and 0.4, are shown in Fig.4-a. The hyperbolic form of the χ^{-1} curve is typical of ferrimagnetic behavior in the Weiss molecular field approximation with two sublattices.

In $(Mg^{2+}_xMn^{2+}_{1-x})_A[Mn_2^{3+}]_BO_4$, the non magnetic Mg^{2+} ions replace the Mn^{2+} ions (S = 5/2) in the tetrahedral site (A), the octahedral site (B) remaining completely occupied by the Mn^{3+} ions (S = 2). The temperature dependence of the inverse paramagnetic susceptibility χ^{-1} can be fitted by equation (1) (ref. 3)

$$\frac{1}{\chi} = \frac{T}{C} + \frac{n}{C^2}\left[C_A^2\alpha + C_B^2\beta + 2C_AC_B\right] - n^2\frac{C_AC_B}{C^3}\frac{\left[C_A - C_B - C_A\alpha + C_B\beta\right]^2}{\left[T - \frac{nC_AC_B}{C}(2-\alpha-\beta)\right]} \quad [1]$$

where C_A and C_B are the Curie constants for the A and B sublattices and $C = C_A + C_B$ corresponds to the total Curie-Weiss constant. In the triangular arrangement, spins at the A sublattice are parallel and those on the two B sublattices are canted at an angle ψ with respect to the direction of the A spins. This model, proposed by Lotgering (7), is equivalent to Néel's two-sublattice model. According to the ionic formula $(Mg^{2+}_xMn^{2+}_{1-x})_A[Mn_2^{3+}]_BO_4$, the Curie constants are assumed as $C_A = (1-x)C_{Mn2+}$ and $C_B = 2C_{Mn3+}$, with $C_{Mn2+} = 4.37$ emu.K/mol and $C_{Mn3+} = 3.03$ emu.K/mol. The constants n, α and β have been treated as adjustable parameters and give the molecular field constants $n = \lambda_{AB}$, $n\alpha = \lambda_{AA}$ and $n\beta = \lambda_{BB}$ between the A and B sites and are related to the exchange constants J_{ij} via equation (2) (ref. 3).

$$J_{ij} = \frac{\lambda_{ij} N_j g_i g_j \mu_B^2}{2Z_{ij}} \quad [2]$$

where Z_{ij} is the number of nearest neighbors on the jth sublattice for an ion on the ith sublattice, and N_j is the number of magnetic ions per mol of the jth sublattice. For $(Mg^{2+}_xMn^{2+}_{1-x})_A[Mn_2^{3+}]_BO_4$, $Z_{AA} = 4(1-x)$, $N_A = (1-x)N$ for λ_{AA},, $Z_{BB} = 6$, $N_B = 2N$ for λ_{BB}. Since the number of nearest neighbors Z_{AB} and Z_{BA} are different, the exchange integral J_{AB} was calculated as an average value between J_{AB} and J_{BA} using the equation $J_{AB} = \lambda_{AB}Ng^2\mu_B^2[(1-x)/48 + 1/\{12(1-x)\}]$, N being Avogadro's number. The Curie temperature T_C has been calculated according to equation (3) (ref. 3).

$$T_C = \frac{n}{2}\left\{-(\alpha C_A + \beta C_B) + \left[(\alpha C_A - \beta C_B)^2 + 4C_AC_B\right]^{1/2}\right\} \quad [3]$$

The condition for the stability of the canted arrangement requires $\alpha\beta < 1$ and, if the canted arrangement is more stable than the collinear state, then $\cos\psi < 1$. The low temperature canting angle ψ can be calculated according to the relation derived from Lotgering's model, $\cos\psi = M_A/\beta M_B$ where M_A and M_B are the A and B sublattice magnetizations, $M_A = (1-x)gS_A\mu_B$ and $M_B = 2gS_B\mu_B$ with g = 2, $S_A = 5/2$, and $S_B = 2$. Those parameters fit consistently the experimental temperature dependence of the inverse magnetic susceptibility χ^{-1} up to x = 0.4 (figure 4-a). Table I gives the molecular field constants n, α and β as well as the values of the low-temperature canting angle ψ for $0 \le x \le 0.4$. The values obtained for Mn_3O_4 (x = 0) are consistent with those reported by Srinivasan and Seehra (3) and the canted angle, ψ = 69.9°, agrees well with the experimental value determined from neutron diffraction measurements (9). The exchange constants J_{AA} and J_{AB} are of the same order of magnitude, but much smaller than J_{BB}, in agreement with the canted structure.

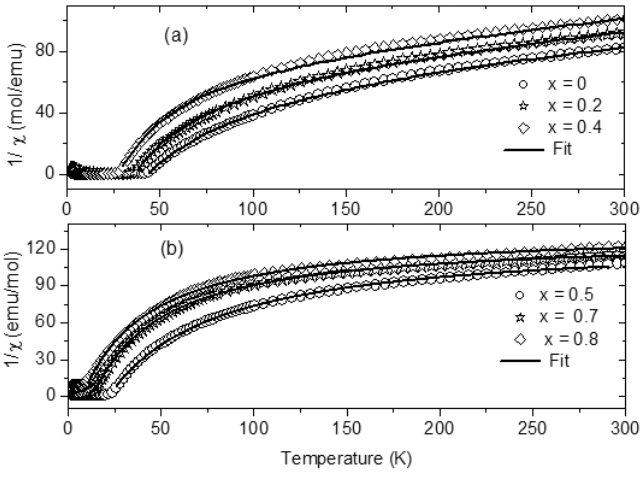

Fig. 4- Inverse magnetic susceptibility of $Mg_xMn_{3-x}O_4$ for : (a) x = 0, 0.2, 0.4 (solid lines show the fit by equation 1), (b) x = 0.5, 0.7, 0.8 (solid lines show the fit by equation 4). Inversa de la susceptibilidad magnética de $Mg_xMn_{3-x}O_4$ para: (a) x = 0, 0.2, 0.4 (las líneas sólidas muestran el ajuste mediante la ecuación [1]), (b) x = 0.5, 0.7, 0.8 (las líneas sólidas muestran el ajuste mediante la ecuación [4]).

TABLA I. MOLECULAR FIELD COEFFICIENTS (N, A, B), INTRASUBLATTICE AND INTERSUBLATTICE EXCHANGE INTEGRALS (J_{AA}, J_{AB}, J_{BB}), CANTING ANGLE AT SATURATION Ψ, CURIE TEMPERATURE T_C, CURIE-WEISS TEMPERATURE Θ_{CW} AND FRUSTRATION PARAMETER $F = \Theta_{CW}/T_C$, DETERMINED FROM EQUATION [1] FOR $MG_XMN_{3-X}O_4$ ($0 \le X \le 0.4$). COEFICIENTES DE CAMPO MOLECULAR (N, A, B), INTEGRALES DE CANJE INTRA-SUBRED E INTER-SUBRED (J_{AA}, J_{AB}, J_{BB}), ÁNGULO DE CANTEADO A SATURACIÓN, Ψ, TEMPERATURA DE CURIE T_C, TEMPERATURA DE CURIE-WEISS Θ_{CW} Y PARÁMETRO DE FRUSTRACIÓN $F = \Theta_{CW}/T_C$, DETERMINADOS A PARTIR DE LA ECUACIÓN [1] PARA $MG_XMN_{3-X}O_4$ ($0 \le X \le 0.4$).

x	C	n	α	β	J_{AA} (K)	J_{AB} (K)	J_{BB} (K)	Ψ (deg)	T_c (K)	Θ_{CW} (K)	f
0	10.43	59.5	0.354	1.78	3.97	-9.31	26.9	69.9	42.6	-307	7.2
0.1	9.99	60.4	0.374	1.75	4.26	-10.10	26.5	71.3	39.0	-336	8.6
0.2	9.55	60.8	0.388	1.71	4.45	-11.21	26.0	73.1	35.2	-408	11.6
0.3	9.12	61.6	0.340	1.68	4.64	-12.37	25.9	74.9	31.9	-434	13.6
0.4	8.68	60.0	0.404	1.64	4.57	-13.65	24.7	76.7	28.5	-510	17.9

As Mg^{2+} increases, the Curie temperature decreases, consistently with the magnetic dilution at the A -site. At the same time, the increase of the canting angle ψ shows an evolution towards an antiferromagnetic coupling between the Mn^{3+} ions at the B-site. For x = 0.5 and above, a discrepancy is observed between the calculated and the experimental susceptibility which might be due to the inadequacy of the two-sublattices model because of the increased magnetic dilution at the A-sublattice. Thus, for samples $0.5 \le x \le 0.9$, we assumed just one magnetic sublattice ; then, the paramagnetic behavior could be fitted by the Curie-Weiss equation (4) which includes a temperature independent paramagnetic contribution χ_{TIP} (Fig. 4-b).

$$1/\chi = (T\text{-}T_C)/(\chi_{TIP}(T\text{-}T_C) + C) \qquad [4]$$

Table II shows a drastic decrease of the Curie temperature as the Mg-content increases from 0.5 up to 0.9. The large negative values of the Curie-Weiss parameter θ_{CW} suggest the existence of strong antiferromagnetic interactions reflected by an increase of the frustration factor f (defined as $f = \theta_{CW}/T_C$) as the Mg-content at the A-site increases.

3.2.2. Cubic domain $1.5 \le x \le 2$

For $x \ge 1.5$, the solid solutions present a cubic structure. In this range, the tetrahedral sites are completely occupied by the Mg^{2+} ions and the additional Mg^{2+} are situated at the octahedral site, giving rise to a mixed valence (Mn^{3+}/Mn^{4+}). Main panel of figure 5 shows the inverse susceptibility, measured at 1 kOe, of some of the cubic samples investigated. The behavior is typical of ferrimagnetic compounds although for the $1.5 \le x \le 1.8$ samples, a deviation from linearity is observed because of a negligible χ_{TIP} contribution (one order of magnitude lower than the case discussed above). At $x \ge 1.9$ and above, the behavior is Curie-Weiss. The parameters derived from the fit to the experimental curves are listed in Table II. The magnetic moments μ_{eff} are similar to the theoretical values μ_{theo} expected for the cationic distribution given by equation (5).

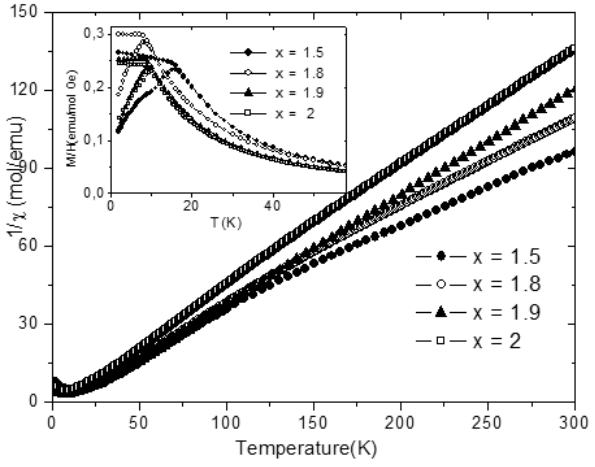

Fig. 5- Inverse magnetic susceptibility, measured at 1 kOe, for samples $Mg_xMn_{3-x}O_4$ in the cubic domain (x = 1.5, 1.8, 1.9, 2). Insert shows the magnetization M/H, measured at 50 Oe, in ZFC and FC modes. Inversa de la susceptibilidad magnética medida a 1 kOe, para muestras $Mg_xMn_{3-x}O_4$ en el dominio cúbico (x = 1.5, 1.8, 1.9, 2). El inserto muestra la magnetización M/H, medida a 50 Oe, en modos ZFC y FC.

$$\mu_{theo} = \sqrt{2(2-x)\mu^2(Mn^{3+}) + (x-1)\mu^2(Mn^{4+})} \qquad [5]$$

Insert, Fig. 5, shows the temperature dependence of the magnetization for x = 1.5, 1.8, 1.9 and 2 under an applied field 50 Oe. An irreversibility of the ZFC and FC curves, typical of a spin-glass, is observed, while the maximum at $T = T_g$ shifts to lower temperatures as the Mg-content increases.

TABLA II. MAGNETIC DATA CALCULATED USING EQUATION [4] FOR ($0.5 \le X \le 0.9$) AND A CLASSICAL CURIE-WEISS EQUATION $X = C/(T\text{-}\Theta_{CW})$ FOR ($1.5 \le X \le 2$).

x	Tc (T_g) K	X_{TIP}, 10^{-3} emu/mol	Θ_{CW} K	f	μ_{eff} μ_B	μ_{theo} μ_B
0.5	20.9	6.08	-539	26	2.53	8.09
0.6	17.2	6.42	-691	40	2.01	7.87
0.7	11.4	6.02	-847	74	1.85	7.65
0.8	5.2	6.53	-849	160	1.67	7.41
0.9	4.0	7.63	-888	222	1.14	7.17
1.5	18	-	-35	-	5.24	5.61
1.6	14	-	-30	-	5.02	5.31
1.7	12	-	-10	-	4.86	4.98
1.8	10	-	5.2	-	4.51	4.64
1.9	11	-	3.0	-	4.41	4.28
2	12	-	-7.0	-	4.33	3.90

4. CONCLUSION

The $Mg_xMn_{3-x}O_4$ compounds have been prepared by a chemical route. The $Mg_xMn_{3-x}O_4$ system undergoes a phase transition from a tetragonal symmetry ($0 \le x \le 0.9$, S.G. $I4_1/amd$) to a cubic symmetry ($1.5 \le x \le 2$, S.G. Fd-3m) across a biphasic domain ($1 \le x \le 1.4$). Upon the substitution of Mn^{2+} ions by Mg^{2+} ions at the tetrahedral site, the ferrimagnetic characteristics decrease drastically in the range $0 \le x \le 0.4$. These results point out that the Mn^{2+} ions at the tetrahedral-site are responsible for the ferrimagnetic order in Mn_3O_4.

Moreover, the partial substitution of Mn^{2+} by a non magnetic ion such as Mg^{2+} modifies the interactions $J_{AA'}$, J_{AB} and J_{BB} so that the long-range ferrimagnetic order evolves into a magnetic frustration state of the B-sublattice, in the range $0.5 \leq x \leq 0.9$. Finally, a spin-glass behavior is observed in the cubic domain for $1.5 \leq x \leq 2$.

REFERENCES

1. S. Kupricka, P. Novak, Oxide Spinels, in Ferromagnetic Materials, edited by E. P. Wohlfarth (North-Holland, Amsterdam, 1982), 3, 189-304 (1982).
2. B. Chardon, F. Vigneron, Mn_3O_4 commensurate and incommensurate magnetic structures, J. Magn. Magn. Mater. 58, 128-134 (1988).
3. G. Srinivasan, M. S. Seehra, Magnetic properties of Mn_3O_4 and a solution of the canted-spin problem, Phys. Rev. B 28, 1-7 (1983).
4. B. Boucher, R. Buhl, M. Perrin, Propriétés et structure magnétique de Mn_3O_4, J. Phys. Chem. Solids 32, 2429-2437 (1971).
5. S. Jacobs, Evidence for triangular moment arrangements in $MO.Mn_2O_3$. J. Phys. Chem. Solids 11, 1-11 (1959).
6. K. Dwight, N. Menyuk, Magnetic Properties of Mn_3O_4 and the Canted spin Problem, Phys. Rev. 119, 1470-1479 (1960).
7. F.K. Lotgering, On the ferrimagnetism of some sulphides and oxides, Phillips Res. Rep. 11,190-249 (1956).
8. G. Jensen, O. Nielsen, The magnetic structure of Mn_3O_4 (Hausmannite) between 4.7 K and the Néel point, 41 K, J. Phys. C 7, 409-424 (1974).
9. A. Kuriki, Y. Moritomo, S. Xu, K. Ohoyama, K. Kato, A. Nakamura, Diffuse scattering due to Geometrical frustration in Mn_3O_4, J. Phys. Soc. Jpn, 72, 458-459 (2003).
10. J. E. Greedan, Geometrically frustrated magnetic materials, J. Mater. Chem., 11, 37-53 (2001).
11. L. Malavasi, P. Ghigna, G. Chiodelli, G. Maggi, G. Flor, Structural and Transport Properties of $Mg_{1-x}Mn_xMn_2O_{4\pm\square}$ Spinels, J.Solid State Chem. 166, 171-176 (2002).

Recibido: 31.07.07
Aceptado: 20.12.07